International Journal of Reconfigurable and Embedded Systems (IJRES)
Vol. 15, No. 2, July 2026, pp. 468~478
ISSN: 2089-4864, DOI: 10.11591/ijres.v15.i2.pp468-478

Design of a flexible modified rectangular dual-band antenna for ISM bands with SAR analysis

Mohan Chinnasamy[1], Uma Mariappan[2], Charulatha Gopinathan[3], Ashokkumar Mani[4], Anita Daniel[2], Sree Devi Baskaran[1]

[1]Department of Electronics and Communication Engineering, St. Joseph's Institute of Technology, Chennai, India
[2]Department of Electronics and Communication Engineering, Sri Sai Ram Engineering College, Chennai, India
[3]Department of Electronics and Communication Engineering, Saveetha School of Engineering, SIMATS, Chennai, India
[4]Department of Electronics and Communication Engineering, Chennai Institute of Technology, Chennai, India

Article Info

Article history:

Received Jan 30, 2026
Revised Mar 20, 2026
Accepted May 30, 2026

Keywords:

Combined slots
Dual band
Industrial, scientific, and medical band
Patch antenna
Specific absorption rate

ABSTRACT

Regarding dual industrial, scientific, and medical (ISM) band utilization, a planar, high-gain, dual-band modified antenna has been implemented application. This modified antenna features a rectangular patch with combined slots. This antenna has a profile of approximately 0.25 λ_0×0.18 λ_0. The combination of slots and modified rectangular patch allows for multiple-band performance. The designed antenna operates in two bands: 5.81 GHz and 2.42 GHz wireless body area network (WBAN). The antenna offered maximum radiation efficiencies of 76.4% and 82.8% in the two operating bands, with peak gains of 3.43 dB and 3.81 dB. The suggested antenna has reflection coefficients of -28.3 dB at 2.43 GHz and -23.9 dB at 5.81 GHz, respectively. The antenna's safety features were additionally evaluated employing a three-layer human body phantom initiated of fat, muscle, and skin tissues. The specific absorption rate (SAR) of the proposed antenna was evaluated using a three-layer human tissue model representing skin, fat, and muscle. The calculated SAR values were analysed according to the IEEE C95.1-1999 and IEEE C95.1-2005 safety guidelines, and the results confirm that the antenna operates within the permissible exposure limits. The measured results closely match simulations, demonstrating its reliability. Owing to its compact size, improved efficiency, strong impedance performance, and validated safety compliance, the proposed antenna is much impressed for effective ISM band communications.

Corresponding Author:

Mohan Chinnasamy
Department of Electronics and Communication Engineering, St. Joseph's Institute of Technology
Chennai, Tamil Nadu, 600119, India
Email: mohanrc803@gmail.com

1. INTRODUCTION

The internet of things (IoT), wireless sensor networks (WSNs), and wireless body area networks (WBANs) are manifestations technologies for wireless communications which have grown significantly in recent decades. These technologies operate in the industrial, scientific, and medical (ISM) frequency bands with vast applications. The availability of unlicensed frequency bands in the 2.4 GHz and 5 GHz ranges has resulted in the development of compact, low-cost, and energy-efficient wireless devices that can be used in a variety of applications, including smart environments, healthcare, industrial applications, and wearable electronics [1], [2]. In such cases, the antenna design must include dual-band functioning, compactness, radiation characteristics, and adequate gain while consuming minimal power. Particularly in WBAN and

wearable IoT scenarios, antennas perform in very close proximity with the human body, making electromagnetic safety and specific absorption rate (SAR) compliance critical design considerations.

For ISM band applications, numerous dual-band and multi-band antenna topologies have been developed [3]–[6]. Multi-band functioning has been achieved using slot loading, meandering, fractals, modified ground structures, multi-feed setups, and the application of metamaterial structures. There are certain restrictions even if these structures have been effectively applied to achieve multi-band functioning for ISM bands. For an instance, in order to achieve multi-band functioning, certain antennas increase the area and/or complexity of the structures. In a similar vein, some antennas achieve compact layouts at the expense of their efficiency and gain. Additionally, even if some researchers have concentrated on antenna bandwidth increase, the radiation stability and antenna matching for the two ISM bands have not received enough attention. Future research for IoT and WBAN applications should focus on the evaluation of the SAR and the interface with the human body, as these topics have not received enough attention in the literature [7].

The antennas must also fulfil a number of performance requirements in order to meet the demands of contemporary IoT, WSN, and WBAN technologies [8], [9]. These requirements include physical dimensions for simple system integration, high battery efficiency, gain for connectivity, stability for dual-band operation at 2.4 GHz and 5.8 GHz, and compliance with various international standards for safe electromagnetic field exposure. Designing an antenna with all these specifications in a straightforward planar shape is still difficult, though. While performance-enhancing approaches can raise the antenna's total cost and structural complexity, decreasing the antenna size through downsizing techniques frequently results in a fall in gain and radiation efficiency. Due to detuning and absorption effects, the design requirements for the antenna perform with the human body will also provide a number of challenges. There is still a great need for an optimized antenna design that satisfies every need for the upcoming generation of wireless systems. Therefore, it is clear that there is a research gap in developing a small, structurally straightforward dual-band antenna with high radiation efficiency and gain while guaranteeing SAR safety for body-centric and IoT-based wireless systems [10]–[13].

For WLAN, IoT, WSN, and WBAN applications, the design offers a thorough and effective antenna layout [14]–[17]. Flexibility and SAR assessment are critical design factors for antennas utilized in ISM band applications, particularly for wearable and human-centric wireless communication systems such as WBAN [18]. The suggested flexible antennas are designed to function in contexts where the antenna deforms under specific circumstances as well as on curved surfaces. Wireless antennas for flexible and human-centric wireless communication systems function in close proximity to the human body. In this scenario, the body's tissues will absorb some of the electromagnetic energy that is conveyed [19]. Consequently, assessing the SAR becomes crucial to guaranteeing the security and functionality of wireless antennas utilized for ISM band applications. The use of SAR evaluation criteria during antenna design ensures the safety and performance of wireless antennas used in ISM band applications.

A dual-band enhanced antenna at 4.9 GHz and 6.7 GHz has been discovered to boost connectivity flexibility, however it does not directly address the 2.4 GHz ISM band, which is often utilized, and may also have downsizing concerns for IoT applications [20]. In order to address band congestion, a wideband triangular antenna has been constructed for 2.31-4.42 GHz employing slotting; nevertheless, these wideband antennas may potentially have problems with selectivity and potential interference from nearby bands [21]. The antenna offers improved gain and bandwidth and dual-band performance at 1.7-2.5 GHz and 5.4-5.9 GHz bands when three transmission lines (TTLs) are used; nevertheless, the multi-line feeding mechanism increases manufacturing complexity and total design cost [22]. Although the Cantor square fractal antenna has demonstrated dual-band performance with 42% and 20% bandwidth in the 2.3-3.6 GHz and 5.1-6.2 GHz bands, its size of $60\times60\times0.813$ mm³, is comparatively larger than that of tiny wireless devices [23]. Similarly, a UWB antenna was designed for wireless capsule endoscopy applications, and the antenna demonstrated dual-band performance at 5.71-6.28 GHz and 8.13-8.58 GHz bands using a circular patch antenna and a cross-slot, as well as a defective ground structure, but the frequency bands are application-specific and do not completely match the standard frequency bands [24]. While many research concentrate on multiband operation with decreased size and increased gain [25]–[33], it is still difficult to achieve high gain and wide bandwidth at the same time in a compact structure because radiation efficiency and impedance performance are frequently compromised by downsizing. Multi-feed designs can increase design complexity and have an impact on structural compactness, even if they have occasionally demonstrated better performance and simpler construction [34], [35]. Thus, it remains a crucial design problem to preserve tiny antenna dimensions while attaining sustained high gain, wide bandwidth, and efficient emission.

The study proposes a novel design for a combined slotted rectangular patch antenna suited for dual-band ISM applications. The recommended antenna performed well in the ISM bands of 2.43 GHz and 5.81 GHz. The reduction of backward radiation is analysed by using the full ground plane. The antenna's designed findings are appropriate for usage in WBAN applications. This work is arranged as section 2 reveals the suggested antenna's physical structure. In section 3, the developed antenna is experimentally validated by implementing the important simulation results. Section 4 presents the key features and developments of the

designed antenna. The SAR analysis is described in section 5. Section 6 contains the results and discussion. The conclusion of this paper is in section 7.

2. DESIGN METHOD

Because of its simplicity, ease of design, and expected resonance, the suggested antenna design uses a rectangular microstrip patch antenna. Dual-band functioning is accomplished through the use of slot antennas, which provide a second resonance with the same antenna size. A polytetrafluoroethylene (PTFE) substrate is selected for its low loss, stability, and flexibility, which enable more efficiency than other substrate in wearable technology applications. In order to achieve the best dual-band performance and guarantee safety, the antenna's design is based on an organized and iterative process. It is initiated by setting the ISM band target frequency (2.4 GHz and 5 GHz). The selection of a suitable PTFE substrate is then made for ensuring low-loss characteristics and flexibility. Initial values for the rectangular patch size are determined using equations for the transmission line model. Verification is done using single-band simulation, as shown in Figure 1. Slot structures are then incorporated for altering the surface current distribution for achieving a second resonance for dual-band characteristics. The fundamental performance characteristics such as S_{11}, gain, and radiation performance are analyzed, followed by a SAR analysis using the human phantom model responsible to the antenna's safe operation on the body.

Figure 1. Flow diagram of the proposed antenna design

The suggested dual-band antenna's structure and arrangement are illustrated in Figure 2. In order to achieve resonant frequencies at 2.43 GHz and 5.81 GHz, the antenna uses a slotted rectangular radiating patch powered by a 50 Ω microstrip line. It is made on a substrate that is 22 mm by 31.5 mm in total size and 1.6 mm thick. The ground plane measures 22 mm by 31.5 mm, whereas the radiating patch is 16 mm wide and 14.5 mm long. The microstrip feed line possesses a width of 2.8 mm and a length of 10.5 mm to enable precise impedance matching. Dual-band performance is made possible without increasing the size of the antenna because to the introduction of slot structures, which modify the surface current distribution. A summary of the intricate the geometrical parameters given in Table 1.

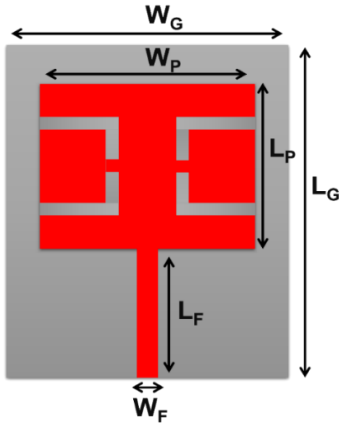

Figure 2. Total geometry and configuration of the antenna

Table 1. Parameter of the proposed antenna

Parameter	Size (mm)	Parameter	Size (mm)
W_G	22.5	L_P	14.5
L_G	31.5	W_F	2.8
W_P	16	L_F	10.5

3. EVOLUTION STAGES

This slotted antenna with the full ground plane is optimised and radiated performance characteristics are evaluated using computer simulation technology (CST-MWS) Suite 2021. Utilizing perfect electric conductor (PEC) with a 0.0354 mm thickness, the ground layer and radiating patch of the estimated antenna are modelled. The substrate is made of PTFE, which is 2 mm thick, has a relative permittivity of 2, and a loss tangent of 0.0009. Open boundary conditions are utilized for analysing the antenna. The antenna's final size of 31.5×22.5×2 mm³ is estimated from the initial dimensions using the fundamental design (1).

$$f_r = \frac{C}{2W_p}\sqrt{\frac{2}{\varepsilon_r+1}} \quad (1)$$

In this expression, *fr* denotes the resonant frequency, *c* is the speed of light in free space, ε_r represents the relative permittivity of the substrate, and W_p corresponds to the width of the radiating patch [36]. Figure 3 depicts the different evolution stages of the proposed antenna configuration. The initial configuration of the antenna is generated by using the fundamental design concepts of a traditional patch antenna with an entire ground plane, as seen in Figure 3(a). At 2.4 GHz, the recommended antenna resonates with a narrow band. In the second stage, four equally sized rectangular strips are etched in rectangular radiating element is given in Figure 3(b). The central frequency of this phase is 4.2 GHz, while its obtained bandwidth is 1.8 GHz. Increasing the number of slots in the patch is required to achieve multi-resonance and minimize the size. Dual band functioning is achieved by extending slots in both side of patch. A full ground plane are aspects of the plain rectangular patch antenna that has been constructed in Figure 3(c).

Figure 3. Different development stages of the suggested antenna; (a) stage 1, (b) stage 2, and (c) stage 3

4. FLEXIBILITY ANALYSIS

Bending physically changes the actual electrical length of the suggested antenna, allowing us to examine its flexibility. For various bending scenarios, scattering characteristics and radiation patterns are investigated through simulation and experimentation. The antenna has been bent with radii of 10 mm, 20 mm, and 30 mm afterwards demonstrating adequate performance in the flat condition has been given in Figure 4. A thorough assessment of the fabricated antenna's flexibility capabilities is made possible by analytical and experimental results showing that it operates steadily when curved along both the x- and y-axes. Figures 4(a) and (b) depict the computed antenna models for x and y axis bending, respectively. A cylindrical foam holder is employed in radiation pattern measurements in the anechoic chamber to sustain the required bending and prevent unwanted flattening of the antenna, allowing for a full examination of the bent radiation patterns.

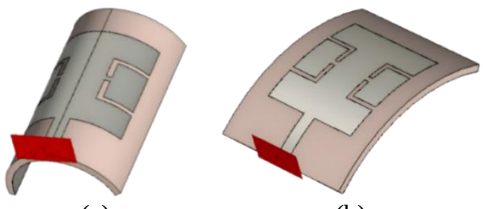

Figure 4. Bending analysis of the proposed antenna; (a) x-axis and (b) y-axis

A simulation of the S-parameter values for bending radiuses of 10 mm, 20 mm, and 30 mm is shown in Figure 5. The findings demonstrate that even during mechanical deformation, the antenna maintains its electromagnetic properties. Resonant responses with slight variations in the resonant frequencies are indicated

by the S_{11} responses at such bending levels. These slight changes are caused by curvature, which modifies the structure's electrical length without affecting impedance matching. According to the simulation results, the impedance bandwidth with the patch bent along the x-axis is between 2.4 GHz and 2.6 GHz, with a slight fluctuation from 2.36 GHz to 2.21 GHz when bent along the y-axis has been displayed in Figures 5(a) and (b). Furthermore, for all bending instances, the S_{21} characteristics verify that isolation stays better than −15 dB throughout the operating spectrum. The main causes of minor discrepancies between simulated and measured data are limits in measuring setup and fabrication errors. Overall, the deliberate bending analysis verifies that the suggested antenna has consistent dual-band performance and significant structural flexibility, rendering it appropriate for conformal and wearable applications.

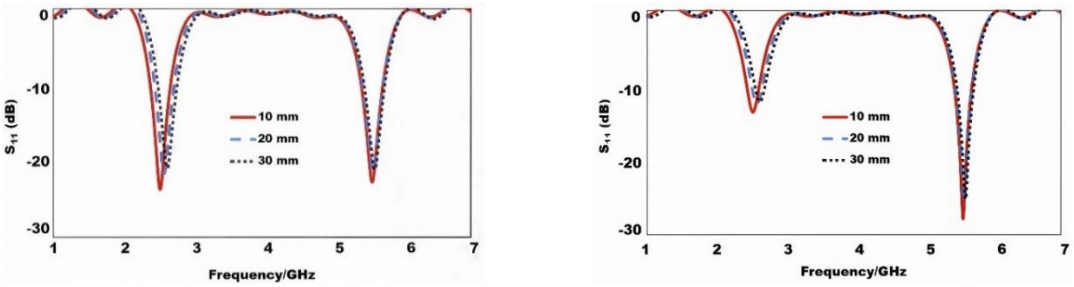

Figure 5. Combined scattering analysis of the proposed antenna at bending conditions; (a) x-axis and (b) y-axis

5. SPECIFIC ABSORPTION RATE ANALYSIS

Figure 6 depicts the simulation environment, which features a multilayer human body phantom with realistic physical proportions. The phantom model's overall dimensions of 80×60×47.7 mm^3 are sufficient to prevent the simulation's electromagnetic boundary condition impacts. The phantom model uses three layers of biological tissues, like the skin, fat, and muscles, to mimic the structural morphology of the human body has been depicted in Figure 6(a). In order to simulate a realistic implantation environment, the fat layer is placed to be the upper boundary of the muscle layer, even though the implantable antennas can be positioned at various depths within the muscle layer. The antenna is situated 2 mm above the muscle layer, and since the skin and fat layers are thought to be 7 mm thick, the total distance is 9 mm and 8 mm above the antenna surface. A thin coating of polyimide superstrate is added to improve biocompatibility and preserve antenna performance by preventing direct contact between the radiating part and the surrounding biological tissue layers. The dielectric properties that have been attributed to the skin, fat, and muscle layers are typical of values that have been routinely published in the ISM frequency band.

The proposed antenna design's simulated peak SAR is 1.95 W/kg, has been depicted in Figure 6(b). This is part of a bigger safety approach in that the tissue environment determines the maximum allowable power to be delivered. The calculated SAR values and corresponding input power that the implanted antenna can use when placed in skin, muscle, and fat tissues in accordance with IEEE C95.1-1999 and IEEE C95.1-2005 specifications are shown in Table 2. The muscular tissue has the greatest SAR levels of 323.5 W/kg (1999) and 57.5 W/kg (2005); therefore, the power delivery is carefully limited to 7.12 mW and 38.76 mW, respectively. The fat tissue allows for more power, 9.05 mW and 44.65 mW, respectively, whereas the skin tissue has lower SAR values of 198.8 W/kg and 30.2 W/kg, with a maximum of 40.1 mW allowed under the 2005 standard.

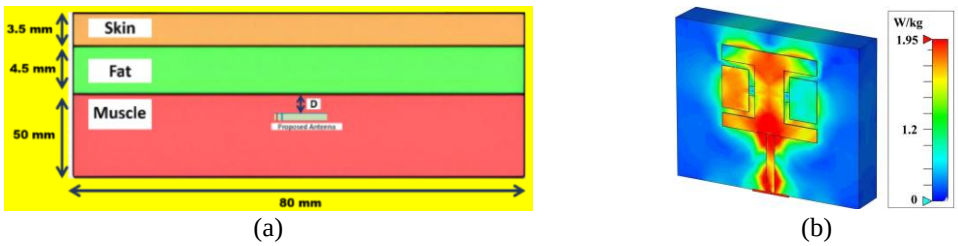

Figure 6. Biological human body tissue model; (a) cross sectional view and (b) SAR distribution

Table 2. Obtained SAR and allowed power at different implant conditions

Phantom model	SAR (W/Kg)		Maximum allowed power (mW)	
	C95.1–1999	C95.1–2005	C95.1–1999	C95.1–2005
Fat	212.3	42.6	9.05	44.65
Muscle	323.5	57.5	7.12	38.76
Skin	198.8	30.2	8.75	40.1

6. RESULTS AND DISCUSSION

The proposed antenna was constructed and put through experimental testing to verify the findings, is illustrated in Figure 7. A vector network analyzer (VNA) was used to test the reflection coefficient, and the findings were examined to confirm the antenna's functionality. The anechoic chamber, an interference-free environment that is appropriately equipped with RF absorbers to reduce reflections, has analysed the radiation pattern measurement. The observed reflection coefficient behaves similarly to the estimated values. Figure 8 depicts a produced prototype and a test configuration for the designed antenna.

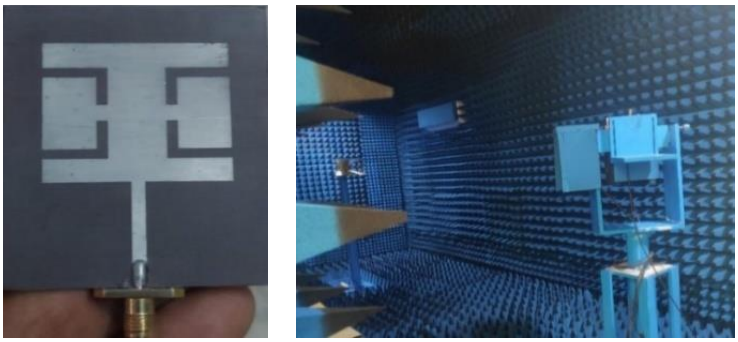

Figure 7. Prototype and measurement setup of the proposed antenna

The antenna offers a bandwidth of around 85 MHz oriented at 2.43 GHz and another of about 100 MHz oriented at 5.81 GHz, according to the simulation outcomes. According to the experiment, the -10 dB bandwidth is centered at 2.4 GHz at around 360 MHz and at 5.8 GHz at about 330 MHz. Figure 8 displays the outcomes of the contrast between the measured and simulated reflection coefficient quantities. The connector cable losses are the reason for the discrepancy. Losses in cables caused by radiation, dielectric losses, and intrinsic resistance. Consequently, it degrades the signal that gets to the antenna, which may result in a reduction in radiation efficiency and a degradationin overall performance. Changes from the proposeddesign parametersduring the process of fabrication can be referred to as fabrication defects. Dimensional issues, material inconsistencies, and assembly faults are a few instances of them. Small physical dimensions and misalignments during assembly can cause changes in resonance frequency, impedance, and radiation properties. Thesecombined effects of cable loss and fabrication faults can cause a large disparity between an antenna's expected performance and actual performance.

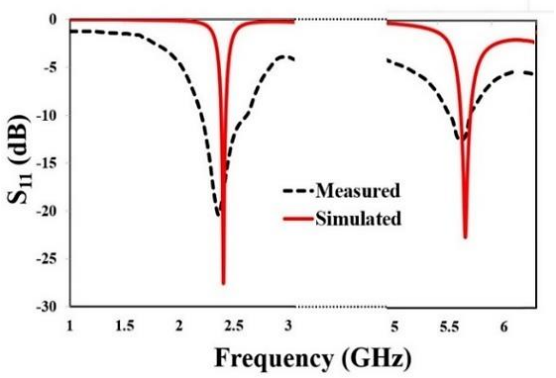

Figure 8. Reflection coefficient plot of the proposed antenna

Figure 9 shows the surface current distribution of the suggested antenna at the 2.4 GHz and 5.8 GHz resonant frequencies. At 2.4 GHz, as shown in Figure 9(a), the current is primarily concentrated near the borders of the radiating patch. In contrast, at 5.8 GHz, depicted in Figure 9(b), the current is mainly distributed around the slots incorporated within the rectangular patch. The suggested antenna's double-band performance is partly attributed to its same-sized slot configuration. These specifications have been observed in the construction and testing of the proposed antenna design.

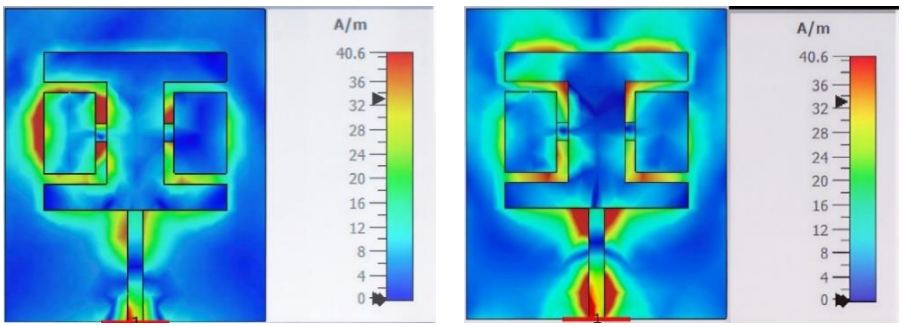

(a) (b)

Figure 9. Surface current density on this antenna; (a) 2.4 GHz and (b) 5.8 GHz

Figure 10 depicts the radiation parameters of the proposed antenna for 2.43 GHz and 5.81 GHz operating frequencies in the xy and xz planes, respectively. Figures 10(a) and (b) show the radiation patterns of the suggested antenna in the xy-plane and xz-plane at operating frequencies of 2.43 GHz and 5.81 GHz, respectively. The suggested antenna exhibits a bidirectional radiation pattern in the xy-plane, according to the examination of the radiation patterns. This suggests that along the xy-plane, the antenna only emits radiation in two directions. The suggested antenna has an omnidirectional radiation pattern in the xz-plane. This suggests that along the xz-plane, the antenna transmits energy in every direction.

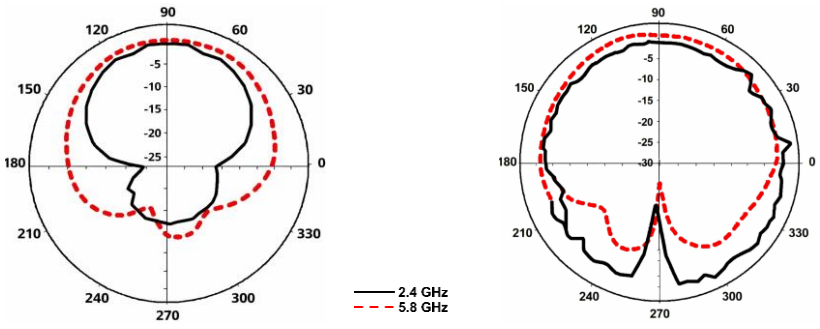

(a) (b)

Figure 10. The compared radiation pattern of the proposed antenna; (a) xy-plane and (b) xz-plane

The varying values of radiation efficiency and peak gain throughout the operating band is depicted in Figure 11. The simulated and measured gains at about 2.0 GHz are about 2.2 dB and 2.0 dB, respectively, with corresponding radiation efficiencies of about 78% and 75%. The gain rises to around 3.52 dB (simulated) and 3.43 dB (measured) at the initial resonant frequency of 2.43 GHz, with radiation efficiencies of nearly 85% and 82%, respectively. The gain decreases to about 2.3 dB (simulated) and 2.2 dB (measured) after 3.5 GHz, with radiation efficiencies of about 76% and 72%, respectively. With radiation efficiencies of around 82% and 79%, respectively, the gain rises to about 3.2 dB and 3.1 dB in the upper band at about 5.0 GHz. The maximal gain peaks to approximately 3.88 dB (simulated) and 3.81 dB (measured) at the second resonating frequency of 5.81 GHz, with high radiation efficiencies of nearly 88% and 85%, respectively. Table 3 gives the overall parametric analysis thoroughly.

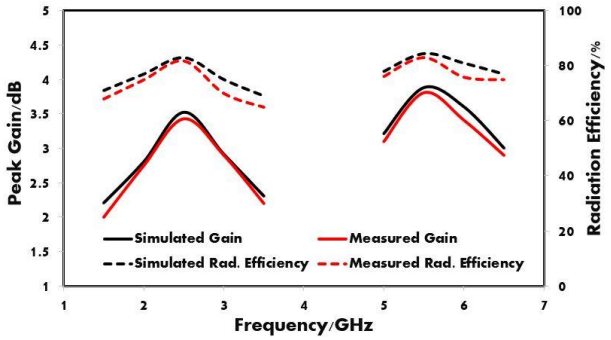

Figure 11. Radiation efficiency and peak gain of the suggested antenna

Table 3. Result analysis of this work

Parameters	Simulation		Measurement	
	2.43 GHz	5.81 GHz	2.43 GHz	5.81 GHz
Reflection coefficients (dB)	-28.3	-23.9	-21.8	-14.4
Bandwidth (MHz)	85	100	360	330
Peak gain (dB)	3.52	3.88	3.43	3.81

Table 4 shows a comparison between the proposed antenna and existing compact dual-band antenna configurations based on their antenna configurations, antenna sizes, substrate materials, and antenna gains. The comparison shows that the proposed antenna design is efficient in reducing the antenna sizes while maintaining high antenna gain for the operating frequency bands.

Table 4. Comparison with previously published dual band antennas

Ref. no.	Antenna type	Antenna size (mm)	Substrate used	Operating frequencies (GHz)	Peak gain (dB)
[25]	Slotted antenna	48×48	FR-4	1.73 and 2.53	-3.8 and 1.9
[26]	PIFA	45×32	FR-4	1.8 and 2.4	1.6 and 1.8
[27]	Monopole antenna	34×26	FR-4	2.4 and 5.2	*Not reported
[28]	Square Slotted antenna	38.5×38.5	Rogers RT5880	2.4 and 2.8	3.4 and 3.2
[29]	Fractal Slotted antenna	50×50	FR-4	3.6 and 5.3	2.78 and 2.32
[30]	Dielectric resonator antenna	120×70	Taconic RF-35	2.46 and 3.5	2.11 and 3.48
[31]	Arch-shaped antenna	47×59.5	FR-4	2.4 and 5.5	1.66 and 3.45
[32]	Flexible antenna	35×20	Rogers Ultralam 3850	2.44 and 5.8	1.13 and 3.17
[33]	Reconfigurable antenna	50×50	*Not reported	3.5 and 5.2	2 and 4
Proposed work	Combined slotted antenna	32.5×22	PTFE	2.43 and 5.81	3.43 and 3.81

7. CONCLUSION

For ISM applications operating at 2.43 GHz and 5.81 GHz, this article developed a small dual-band modified rectangular patch antenna. With reflection coefficients of −28.3 dB and −23.9 dB, radiation efficiency of 78.2% and 83.4%, and maximum gains of 3.43 dBi and 3.80 dBi for 2.43 GHz and 5.81 GHz, respectively, the suggested antenna demonstrated good impedance matching characteristics. When compared to a conventional rectangular patch antenna, the antenna size might be reduced by about 76% using optimized slot elements. The SAR was determined to be within the bounds of IEEE C95.1-1999 and IEEE C95.1-2005 standards using a human tissue model made up of layers of skin, fat, and muscle. The proposed antenna is well suited for flexible IoT applications due to its compact and low-profile design. It maintains stable impedance and radiation characteristics, ensuring reliable wireless communication even in bendable or space-constrained environments. Even though the suggested work makes it clear that the antenna is small and appropriate for applications with modest gain, it is crucial to improve the gain of the suggested antenna for applications requiring long-distance communication.

FUNDING INFORMATION

Authors state no funding involved.

AUTHOR CONTRIBUTIONS STATEMENT

This journal uses the Contributor Roles Taxonomy (CRediT) to recognize individual author contributions, reduce authorship disputes, and facilitate collaboration.

Name of Author	C	M	So	Va	Fo	I	R	D	O	E	Vi	Su	P	Fu
Mohan Chinnasamy	✓	✓		✓	✓	✓		✓		✓			✓	✓
Uma Mariappan		✓	✓		✓	✓	✓	✓	✓		✓		✓	
Charulatha Gopinathan		✓	✓	✓			✓		✓		✓			
Ashokkumar Mani		✓		✓	✓	✓	✓		✓	✓		✓		✓
Anita Daniel		✓		✓	✓	✓		✓		✓		✓		✓
Sree Devi Baskaran	✓	✓	✓	✓	✓	✓		✓	✓				✓	

C : **C**onceptualization
M : **M**ethodology
So : **So**ftware
Va : **Va**lidation
Fo : **Fo**rmal analysis
I : **I**nvestigation
R : **R**esources
D : **D**ata Curation
O : Writing - **O**riginal Draft
E : Writing - Review & **E**diting
Vi : **Vi**sualization
Su : **Su**pervision
P : **P**roject administration
Fu : **Fu**nding acquisition

CONFLICT OF INTEREST STATEMENT

Authors state no conflict of interest.

DATA AVAILABILITY

The authors confirm that the data supporting the findings of this study are available within the article and its supplementary materials.

REFERENCES

[1] Y. F. Liu *et al*., "A Survey of Recent Advances in Optimization Methods for Wireless Communications," *IEEE Journal on Selected Areas in Communications*, vol. 42, no. 11, pp. 2992–3031, 2024, doi: 10.1109/JSAC.2024.3443759.

[2] M. Marzouk *et al*., "Efficient broadband fractal antenna for WiMAX and WLAN," *Heliyon*, vol. 10, no. 5, 2024, doi: 10.1016/j.heliyon.2024.e26087.

[3] S. Yan, X. Zhai, H. Ren, and J. Zhang, "A Low-Profile Dual-Polarized Omnidirectional Antenna for WLAN/UWB Applications," *IEEE Antennas and Wireless Propagation Letters*, vol. 23, no. 5, pp. 1433–1437, 2024, doi: 10.1109/LAWP.2024.3358324.

[4] J. Zhang, "The application of bluetooth technology in the internet of things," *Applied and Computational Engineering*, vol. 12, no. 1, pp. 177–183, 2023, doi: 10.54254/2755-2721/12/20230334.

[5] K. Pahlavan and P. Krishnamurthy, "Evolution and Impact of Wi-Fi Technology and Applications: A Historical Perspective," *International Journal of Wireless Information Networks*, vol. 28, no. 1, pp. 3–19, 2021, doi: 10.1007/s10776-020-00501-8.

[6] I. Natgunanathan, N. Fernando, S. W. Loke, and C. Weerasuriya, "Bluetooth Low Energy Mesh: Applications, Considerations and Current State-of-the-Art," *Sensors*, vol. 23, no. 4, 2023, doi: 10.3390/s23041826.

[7] P. S. Bakariya, S. Dwari, M. Sarkar, and M. K. Mandal, "Proximity-coupled microstrip antenna for bluetooth, WiMAX, and WLAN applications," *IEEE Antennas and Wireless Propagation Letters*, vol. 14, pp. 755–758, 2015, doi: 10.1109/LAWP.2014.2379611.

[8] R. A. Saeed and S. Khatun, "Design of Microstrip Antenna for WLAN," *Journal of Applied Sciences*, vol. 5, no. 1, pp. 47–51, 2005.

[9] J. Yang, H. Wang, Z. Lv, and H. Wang, "Design of miniaturized dual-band microstrip antenna for WLAN application," *Sensors (Switzerland)*, vol. 16, no. 7, 2016, doi: 10.3390/s16070983.

[10] Z. Khan, M. H. Memon, S. Ur Rahman, M. Sajjad, F. Lin, and L. Sun, "A single-fed multiband antenna for WLAN and 5G applications," *Sensors (Switzerland)*, vol. 20, no. 21, pp. 1–13, 2020, doi: 10.3390/s20216332.

[11] D. K. Janapala and M. Nesasudha, "A highly miniaturized antenna with wider band for biomedical applications," *Electromagnetic Biology and Medicine*, vol. 41, no. 1, pp. 35–43, 2022, doi: 10.1080/15368378.2021.1993892.

[12] N. A. Malik, P. Sant, T. Ajmal, and M. Ur-Rehman, "Implantable Antennas for Bio-Medical Applications," *IEEE Journal of Electromagnetics, RF and Microwaves in Medicine and Biology*, vol. 5, no. 1, pp. 84–96, 2021, doi: 10.1109/JERM.2020.3026588.

[13] K. R. Mahmoud and A. M. Montaser, "Design of Multiresonance Flexible Antenna Array Applicator for Breast Cancer Hyperthermia Treatment," *IEEE Access*, vol. 10, pp. 93338–93352, 2022, doi: 10.1109/ACCESS.2022.3203431.

[14] A. A. Ibrahim, W. A. E. Ali, M. Alathbah, and H. A. Mohamed, "A Frequency Reconfigurable Folded Antenna for Cognitive Radio Communication," *Micromachines*, vol. 14, no. 3, 2023, doi: 10.3390/mi14030527.

[15] M. Wei, J. Wang, X. Wang, T. Liu, Y. Lu, and Y. Gao, "Low-Profile Dual-Band Microstrip Patch Antenna With Shorting Pins," *IEEE Antennas and Wireless Propagation Letters*, vol. 23, no. 6, pp. 1834–1838, 2024, doi: 10.1109/LAWP.2024.3370724.

[16] J. Doe and A. Smith, "Design and optimization of dual-band microstrip patch antennas for WLAN applications," *IEEE Transactions on Antennas and Propagation*, vol. 20, pp. 123–134, 2022.

[17] U. Musa *et al.*, "Design and Analysis of a Compact Dual-Band Wearable Antenna for WBAN Applications," *IEEE Access*, vol. 11, pp. 30996–31009, 2023, doi: 10.1109/ACCESS.2023.3262298.

[18] S. J. Yang, W. Duan, Y. Y. Liu, H. Ye, H. Yang, and X. Y. Zhang, "Compact Dual-Band Base-Station Antenna Using Filtering Elements," *IEEE Transactions on Antennas and Propagation*, vol. 70, no. 8, pp. 7106–7111, 2022, doi: 10.1109/TAP.2021.3083727.

[19] C. Zhao and W. Geyi, "Design of a dual band dual mode antenna for on/off body communications," *Microwave and Optical Technology Letters*, vol. 62, no. 1, pp. 514–520, Jan. 2020, doi: 10.1002/mop.32085.

[20] S. Ahmad, A. Ghaffar, N. Hussain, and N. Kim, "Compact dual-band antenna with paired l-shape slots for on-and off-body wireless communication," *Sensors*, vol. 21, no. 23, 2021, doi: 10.3390/s21237953.
[21] F. Khajeh-Khalili, A. Shahriari, and F. Haghshenas, "A simple method to simultaneously increase the gain and bandwidth of wearable antennas for application in medical/communications systems," *International Journal of Microwave and Wireless Technologies*, vol. 13, no. 4, pp. 374–380, 2021, doi: 10.1017/S1759078720001075.
[22] A. Al Ka'bi, "Design of a Microstrip Dual Band Fractal Antenna for Mobile Communications," *Telecommunications and Radio Engineering (English translation of Elektrosvyaz and Radiotekhnika)*, vol. 82, no. 4, pp. 61–77, 2023, doi: 10.1615/TELECOMRADENG.2023044473.
[23] M. T. Yassen, M. R. Hussan, H. A. Hammas, H. Al-Saedi, and J. K. Ali, "A Dual-Band Printed Antenna Design Based on Annular Koch Snowflake Slot Structure," *Wireless Personal Communications*, vol. 104, no. 2, pp. 649–662, 2019, doi: 10.1007/s11277-018-6039-0.
[24] A. Arif, M. Zubair, M. Ali, M. U. Khan, and M. Q. Mehmood, "A Compact, Low-Profile Fractal Antenna for Wearable On-Body WBAN Applications," *IEEE Antennas and Wireless Propagation Letters*, vol. 18, no. 5, pp. 981–985, 2019, doi: 10.1109/LAWP.2019.2906829.
[25] M. Wang, L. Yang, and Y. Shi, "A dual-port microstrip rectenna for wireless energy harvest at LTE band," *AEU - International Journal of Electronics and Communications*, vol. 126, 2020, doi: 10.1016/j.aeue.2020.153451.
[26] L. Chen, H. Zhang, Z. Chen, Y. Zhang, J. Yao, and Y. Xing, "Design of low-profile dual-band antenna for IoT applications," in *2019 IEEE 3rd International Conference on Electronic Information Technology and Computer Engineering, EITCE 2019*, 2019, pp. 1805–1809, doi: 10.1109/EITCE47263.2019.9095024.
[27] L. Wang, J. Chen, Y. Ping, L. Han, and W. Zhang, "Design of a Dual-band Monopole Antenna for WLAN Applications," in *2019 Computing, Communications and IoT Applications (ComComAp 2019)*, 2019, pp. 167–169, doi: 10.1109/ComComAp46287.2019.9018847.
[28] W. M. Abdulkawi, A. F. A. Sheta, I. Elshafiey, and M. A. Alkanhal, "Design of Low-Profile Single- and Dual-Band Antennas for IoT Applications," *Electronics*, vol. 10, no. 22, p. 2766, Nov. 2021, doi: 10.3390/electronics10222766.
[29] O. Benkhadda *et al.*, "Compact Broadband Antenna with Vicsek Fractal Slots for WLAN and WiMAX Applications," *Applied Sciences (Switzerland)*, vol. 12, no. 3, 2022, doi: 10.3390/app12031142.
[30] A. Altaf and M. Seo, "Dual-band circularly polarized dielectric resonator antenna for wlan and wimax applications," *Sensors (Switzerland)*, vol. 20, no. 4, 2020, doi: 10.3390/s20041137.
[31] E. M. Salah, H. A. Atallah, A. Abdelaziz, H. A. Mohamed, and E. K. I. Hamad, "Radiation Pattern Reconfigurable Arch-Shaped Dual-Band Antenna for Wi-Fi and WLAN Applications," *Advanced Electromagnetics*, vol. 13, no. 1, pp. 33–38, 2024, doi: 10.7716/aem.v13i1.2258.
[32] M. Kadry, M. El Atrash, and M. A. Abdalla, "Design of an Ultra-thin Compact Flexible Dual-Band Antenna for Wearable Applications," in *2018 IEEE Antennas and Propagation Society International Symposium and USNC/URSI National Radio Science Meeting, APSURSI 2018 - Proceedings*, 2018, pp. 1949–1950, doi: 10.1109/APUSNCURSINRSM.2018.8609247.
[33] N. Sathishkumar, S. Divya, D. R. P. Rajarathnam, P. G. Ayyavu, and P. Radhakrishnan, "Design of Asymmetrically Loaded Dual Band Antenna for ISM Band Applications," *SN Computer Science*, vol. 5, no. 5, 2024, doi: 10.1007/s42979-024-02910-5.
[34] C. Mohan, J. Silamboli, S. Divya, and R. S. Sheela, "A Compact Inset Coupled-Fed Triangular Patch Antenna For Wideband 5G Applications," *Indonesian Journal of Electrical Engineering and Informatics*, vol. 12, no. 3, pp. 659–666, 2024, doi: 10.52549/ijeei.v12i3.5677.
[35] K. Sreelakshmi, G. S. Rao, and M. N. V. S. S. Kumar, "A compact grounded asymmetric coplanar strip-fed flexible multiband reconfigurable antenna for wireless applications," *IEEE Access*, vol. 8, pp. 194497–194507, 2020, doi: 10.1109/ACCESS.2020.3033502.
[36] C. A. Balanis, *Antenna theory: analysis and design*, 4th ed. John Wiley & Sons, 2016.

BIOGRAPHIES OF AUTHORS

Mohan Chinnasamy is working as assistant professor in Department of Electronics and Communication Engineering, St. Joseph's Institute of Technology, Tamil Nadu, India. He has completed Ph.D. in planar antenna in the Department of Electronics and Communication Engineering at Sri Sivasubramaniya Nadar College of Engineering, Anna University, India. He has received his B.E. in electronics and communication engineering from Peri Institute of Technology, Anna University, Chennai, Tamil Nadu, India in 2015 and completed his M.E. communication systems in Sri Venkateshwara College of Engineering, Anna University, Chennai, Tamil Nadu, India in 2017. His research area interests are microwave components like antennas, metamaterials, and electromagnetic bandgap structures. He can be contacted at email: mohanrc803@gmail.com.

Uma Mariappan is an assistant professor in the Department of ECE at Sri Sairam Engineering College, Chennai. She completed her Master of Engineering (M.E.) in communication systems and is currently pursuing her Doctor of Philosophy (Ph.D.) at Anna University, Chennai. Her research interests encompass antenna design, electromagnetic fields, microwave engineering, and next-generation wireless communication systems. Her recent work focuses on designing and optimizing planar multi-band MIMO antennas for 5G and beyond, specifically targeting applications at millimetre-wave frequencies. She can be contacted at email: uma.ece@sairam.edu.in.

Charulatha Gopinathan was born on August, 1979 in Chennai, Tamil Nadu. She received her Bachelor's degree in Electronics and Communication Engineering from Rajalakshmi Engineering College, Chennai in 2001, Master's degree in applied electronics from Sathyabama Institute of Science and Technology, Chennai in 2011 and she was awarded doctorate degree in information and communication engineering from Anna University, Chennai in 2018. She is presently an associate professor in the Department of Electronics and Communication Engineering, Saveetha School of Engineering, SIMATS, Chennai, India. Her research interests include signal processing, image processing, IoT and microwave, neural networks, and communication systems. She can be contacted at email: drcharulatha79@gmail.com.

Ashokkumar Mani was born on April 1985 in Chennai, Tamil Nadu, India. He received his Bachelor's degree in electronics and communication engineering from GKM College of Engineering and Technology, Anna University, Chennai in 2009, Master's degree in Communication Systems from GKM College of Engineering and Technology, Anna University, Chennai in 2012. He is currently an assistant professor in the Department of Electronics and Communication Engineering at Chennai Institute of Technology, Chennai. His research interests include internet of things and microwave design. He can be contacted at email: ashoktharan12@gmail.com.

Anita Daniel received her Bachelor's degree in Electronics and Communication Engineering from Annai Mathammal Sheela Engineering College, Namakkal, Tamil Nadu, India in 2001. She received Master's degree in applied electronics from Hindustan College of Engineering, Anna University, Chennai, Tamil Nadu, India in 2004 and her Ph.D. in 2022 from Sathyabama Institute of Science and Technology, Chennai, Tamil Nadu, India. She is currently working as an associate professor in the Department of Electronics and Communication Engineering, Sri Sai Ram Engineering College, Chennai, Tamil Nadu, India. Her major areas of interest are wireless sensor networks, cryptography, and VLSI design. She can be contacted at email: d.anitaedwin@yahoo.com.

Sree Devi Baskaran is an assistant professor in the Department of Electronics and Communication Engineering, St. Joseph's Institute of Technology, Tamil Nadu, India. She completed her Master of Engineering (M.E.) in communication systems and is currently pursuing her Doctor of Philosophy (Ph.D.) at Anna University, Chennai. Her research interests encompass antenna design, filter design, microwave engineering, and 6G communication. Her most recent work involves the design and optimization of flexibleantennas for 5G and beyond, with a particular emphasis on health-careapplications. She can be contacted at email: sreedevistjoseph@gmail.com.